nature communications

Article

https://doi.org/10.1038/s41467-024-51764-1

Hydrogen bonding template enables remote *meta*-C–H alkenylation of nitroarenes with electron-deficient alkenes

Received: 28 January 2024

Accepted: 19 August 2024

Published online: 30 August 2024

Check for updates

Bishal Dutta[1], Mayank Mahajan[2], Animesh Ghosh[1], Maciej Dajek[3], Rafal Kowalczyk[3] ✉, Bhaskar Mondal[2] ✉, Haibo Ge[4] ✉ & Debabrata Maiti[1] ✉

Regioselective distal C–H functionalization of nitroarenes by overriding proximal C–H activation has remained an unsolved challenge. Herein, we present a palladium-catalyzed *meta*-C–H alkenylation of nitroarene substrate, achieved through leveraging the non-covalent hydrogen bonding interactions. Urea-based templates comprising an elongated biphenyl linker designed in such a way that it interacts with nitro group via strong hydrogen bonding interaction, while a cyano based directing group is attached along the template to coordinate with the palladium center, thereby facilitating the activation of the remote *meta*-C–H bond of nitrobenzene. Computational mechanistic investigation and the analysis of non-covalent interaction deciphers the crucial role of H-bonding in regulating the regioselectivity.

The covalent directing group and transient directing group (TDG) assisted remote (*meta*/*para*) C–H functionalization strategy in the realm of palladium catalysis, has been extensively researched over the past decades[1–8]. While these methods have partially addressed the issue of regioselectivity, they unavoidably introduce extra steps for the installation and subsequent removal of the directing group after modification. This added complexity inevitably undermines the step and atom economy of the reaction. Most importantly these directing templates cannot be installed with a number of organic substrates like nitrobenzene. To address these challenges, there has been a significant surge of interest to merge the concept of non-covalent interactions with transition metal catalysis in the recent years[9,10]. Harnessing the weak non-covalent interactions to functionalize distal C–H bonds has been widely investigated in the field of iridium-catalyzed borylation[11–15]. The weaker nature of non-covalent interaction results in more flexible transition states, making it challenging to differentiate a specific C–H bond for activation[16]. In 2021, Jin and co-workers demonstrated a hydrogen bonding methodology under palladium catalysis for the alkenylation of carbonyl-based arene substrates at the distal *meta* position (Fig. 1b)[17]. Recently, in 2023, our group reported the palladium-catalyzed *meta*-C–H alkenylation of aromatic long-chain amines with the aid of an anionic H-bond acceptor template (Fig. 1a)[18]. Simultaneously, van Gemmeren and co-workers utilized the concept of electrostatic interaction between the substrate and ligand to enable *meta*- alkenylation of benzyl ammonium salts (Fig. 1a)[19]. In this study, we present an approach to achieve distal *meta*-C–H alkenylation of highly electron deficient nitroarene substrate through the strategic implementation of urea-based hydrogen bonding concept (Fig. 1c). Nitroarenes, characterized by the pronounced electron deficiency, pose formidable challenges in achieving site-selective C–H activation due to unfavorable redox interactions with palladium[20]. The compelling electron-withdrawing properties inherent to the nitro group promotes ring substitution at *meta* position, confined to the limited domain of SNAr type reactions[21,22]. Moreover, the coordinating ability of nitro group with transition metals prefer selective *ortho*-C–H activation[23,24]. Therefore, by overriding the intrinsic challenges associated with nitro group, we unveil an unexplored avenue for accessing *meta*-alkenylated nitroarene derivatives.

[1]Department of Chemistry, Indian Institute of Technology Bombay, Mumbai, India. [2]School of Chemical Sciences, Indian Institute of Technology Mandi, Kamand, Himachal Pradesh, India. [3]Wroclaw University of Science and Technology, Wroclaw, Poland. [4]Department of Chemistry and Biochemistry, Texas Tech University, Lubbock, TX, USA. ✉e-mail: rafal.kowalczyk@pwr.edu.pl; bhaskarmondal@iitmandi.ac.in; haibo.ge@ttu.edu; dmaiti@iitb.ac.in

https://doi.org/10.1038/s41467-024-51764-1

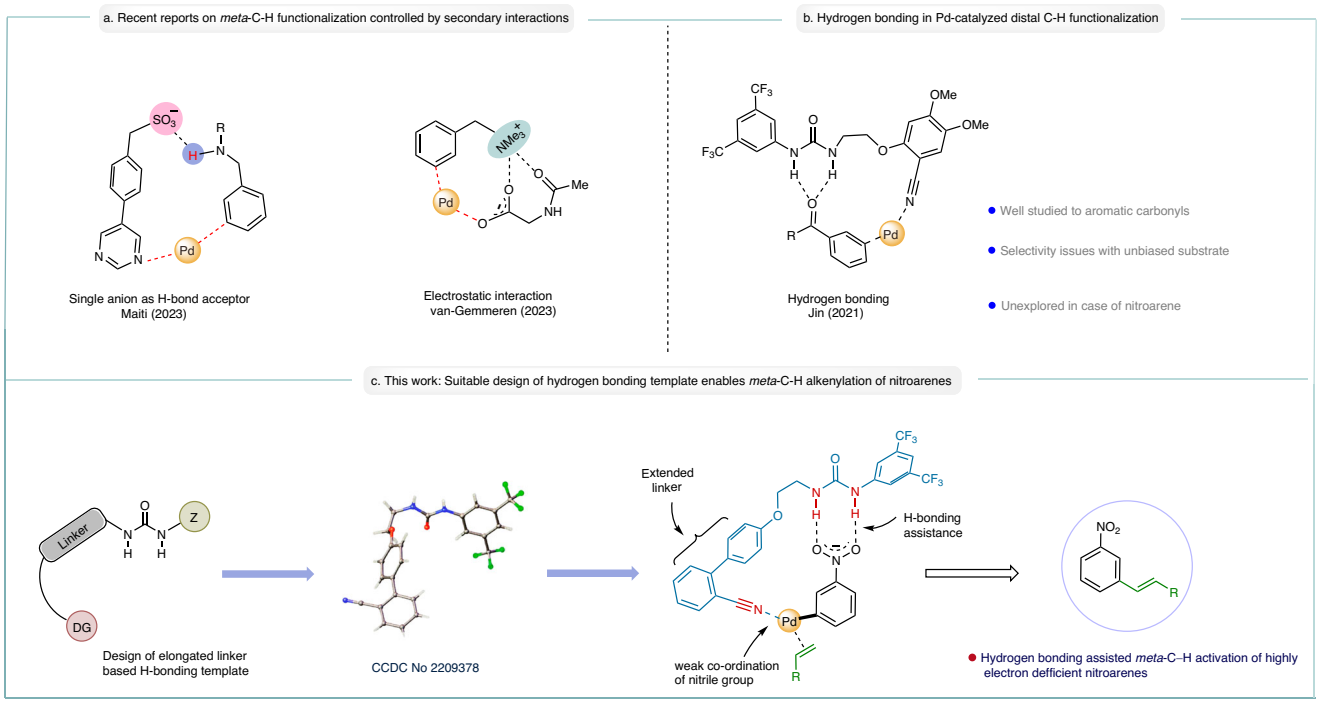

Fig. 1 | Distal C–H alkenylation by non-covalent interactions. a Recent reports on *meta*-C–H functionalization controlled by non-covalent interactions. **b** Pd-catalyzed olefination of aromatic carbonyls by hydrogen bonding. **c** Present work: A suitable design of H-bonding template enables *meta*-C–H alkenylation of nitroarenes and aromatic carbonyls.

Results

Optimization of the H-bonding templates

We recognized that the H-bonding template required three components; (1) H-bond donor, i.e., urea/thiourea thiourea/squaramide core interacting with the nitro group through hydrogen bonding, (2) a directing group coordinating to the palladium center, (3) a suitable spacer acting as a bridge between donor and directing group ensuring the regioselectivity of the C–H activation. This interpretation leads us to first synthesize a hydrogen bond donor template (**HT1**; Fig. 2), encompassing an urea motif, nitrile directing group and a biphenyl linker in between. We hypothesized that the introduction of a biphenyl motif as an elongated linker perhaps will assist in bringing the palladium center closer to the *meta* C–H bond of nitrobenzene. In our initial studies, we obtained a selective *meta*-alkenylated product of nitrobenzene substrate with 30% yield and 3:1 selectivity (*meta* : *others*) using **HT1** as the H-bonding template. Following this hypothesis, later we synthesized a vast array of H-bond donor templates, altering the position of phenyl ring containing nitrile directing group and also by changing the mode of H-bonding interaction (**HT2**-**HT10**; Fig. 2). We observed an improvement in yield and regioselectivity when **HT3** was used as the H-bonding template. The desired *meta*-alkenylated product formed with 44% yield with 6.5:1 *meta*-selectivity (Fig. 2). The selectivity originates from the specific orientation of the hydrogen bonded template with respect to the substrate scaffold in the transition state, as revealed through our density functional theory (DFT)-based calculations (*vide infra*). Only a trace amount of *meta*- alkenylated product was formed when a thiourea-based template was used (**HT4**). This is likely due to the poisoning of palladium catalyst by the sulfur center present in the thiourea template (Fig. 2)[25]. Subsequently, we studied a series of squaramide-based templates **HT5**-**HT10** (Fig. 2) having different geometry of H-bonding unit, albeit exhibiting properties to bind palladium through M–O=C interactions. Although enhanced N–H acidity resulting in stronger H-bonding with the substrate, the complexation of palladium resulted in no reaction. We have also synthesized another template **HT11** (Fig. 2) by increasing the linker length of the carbon chain between biphenyl directing group and urea motif. However, we haven't noticed any improvement of the results in comparison to **HT3**. It was also observed that the yield and selectivity reduced significantly in the presence of a strong coordinating pyridine-based H-bonding template (**HT12**). The introduction of carboxylic acid as a directing group in the template (**HT13**) also provided poor yield and regioselectivity. Three H-bonding templates (**HT1**-**HT3**) were subjected to computational investigation to decipher the origin of the better selectivity exhibited by template **HT3** (*vide infra*).

Substrate scopes

After a thorough optimization of reaction parameters (Supplementary Tables 1–4, Supplementary Information, Sections 2.2.1–2.2.5), we moved to investigate the generality of this protocol with 10 mol% of $Pd(OAc)_2$, 20 mol% of *N*-Ac-Gly-OH, 90 mol% of H-bonding template, silver acetate (3 *equiv*) as a sacrificial oxidant in HFIP solvent. A diverse range of nitroarenes were found to be compatible under the optimized reaction condition (Fig. 3). Simple nitrobenzene produced *meta*-alkenylated product with 46% yield and 7:1 regioselectivity with this optimized condition (**3a**). *Ortho*-nitro toluene gave desired *meta*-alkenylated product with 51% yield, albeit with a *meta* : *meta'* selectivity of 1.6:1 and *meta* : *others* selectivity of 4:1 (**3b**). In the case of 2-methoxy nitrobenzene substrate, *meta*-alkenylated product was formed with almost exclusive selectivity and moderate yield (**3c**). Similarly, 4-substituted nitroarene like *para*-nitro toluene was successfully alkenylated at *meta* position with an yield of 54% and *meta* : *others* selectivity of 4.5:1 (**3d**). The main reason for reduced selectivity in these substrates is the steric induction provided by the methyl group present in the ring. The introduction of an ethoxy group at the *para* position leads to excellent yield and selectivity (**3e**), indicating that the electronic effect of substituent has a governing role in controlling the extent of hydrogen bonding with the urea-based template (**HT3**). Not only the electron-donating substituents but also the electron-withdrawing group present at the *para* position of nitrobenzene was found to be compatible under this reaction condition (**3f**).

https://doi.org/10.1038/s41467-024-51764-1

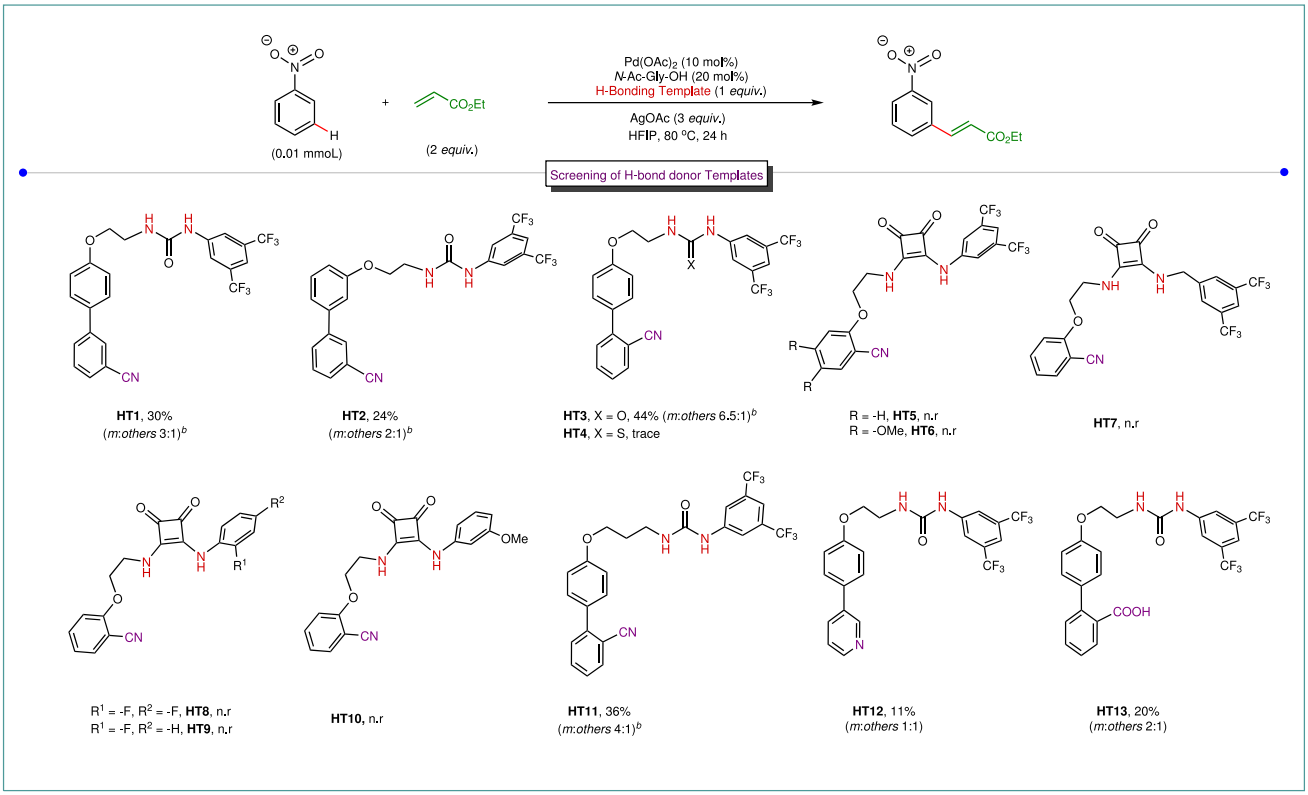

Fig. 2 | Evaluation of H-bond donor templates in *meta*-C–H alkenylation. [a]Yield and regioselectivity was determined by 1H-NMR analysis with reference to 1,3,5-trimethoxy benzene as an internal standard. [b]C–H alkenylation of the template was also observed. n.r no reaction, **HT** Hydrogen bonding template.

Subsequently, we proceeded to explore the fate of this reaction in the case of 2,4-disubstituted nitrobenzene substrates. It was found that the reaction works reasonably well with electronically diverse substituents present at the 2- and 4- positions of the nitroarene ring (**3g**-**3j**). After that, we drew our attention to 2,6-disubstituted nitroarenes. Intriguingly, 2,6-dimethyl nitrobenzene worked well in this reaction despite of having immense steric demand (**3k**). Moderately electron-deficient substrates, like 2,6-difluoro nitrobenzene and 2,6-dichloro nitrobenzene, were also alkenylated selectively at the *meta* position using this approach (**3l** and **3m**). We have observed that the presence of electron donating groups in the nitroarene ring helps to increase the yield as well as regioselectivity of the alkenylated product. As different types of nitro benzenes were found to be suitable under this reaction condition, we started to explore a series of alkenes (Fig. 3). Excitingly, selective *meta*-alkenylated products formed with short to long alkyl chains containing acrylates (**3n**-**3q**). Cyclohexyl acrylate along with dicyclopentanyl acrylate were found to be compatible under this reaction condition furnishing *meta* product with moderate yield and selectivity (**3r** and **3s**). Simple trifluoromethyl acrylate and fluoro-containing long chain acrylate also worked out satisfactorily in this particular reaction (**3t** and **3u**). This protocol was also applicable for activated alkene like methyl vinyl ketone (**3v**) and acrylate-containing natural product core (**3w**). We have also sought to examine the reactivity of other activated alkene like acrylonitrile. It has been observed that acrylonitrile gives the selective *meta*-alkenylated product with excellent yield and regioselectivity (**3x**). In this particular case, both (*E*) and (*Z*) isomers of the alkenylated product formed with 1.7:1 selectivity.

Mechanistic investigation

In an effort to justify the role of **HT3**, we performed control experiments. When the alkenylation reaction was carried out in absence of the template, the yield as well as selectivity of the product remarkably diminished (Fig. 4a). This unambiguously shows participation of **HT3** in this reaction and its ability to activate distal *meta*-C–H bond in preference over the other C–H bonds. To investigate the role of **HT3** further, we synthesized another template (**HT14**) by *N*, *N*-di-methylation of **HT3**. As the two N–H bonds are protected in this case, chance of hydrogen bonding with nitroarene substrate is null. We then performed alkenylation reaction in the presence of this particular methylated template (**HT14**) (Fig. 4a). As expected, under this particular condition, desired *meta*-alkenylated product was not formed. This inspection clearly suggests that hydrogen bonding interaction is essential to be present between substrate and template which is governing the site-selectivity in our alkenylation reaction. Our next objective was to probe the H-bonding interaction between template (**HT3**) and nitrobenzene. In search of this, template **HT3** was dissolved in acetone-*d6* and an equimolar amount of guest molecule, i.e., nitrobenzene was added. After that, NMR spectra was recorded. Interestingly, characteristic peak of two N–H proton present in **HT3** shifted to downfield region (Fig. 4b), signifying hydrogen bonding between nitrobenzene and **HT3**. Considering the important role of HFIP as a solvent in distal C–H functionalization[26], we anticipated that it might play a critical role in hydrogen bonding in our case. So, we performed the NMR experiment in presence of HFIP. This time NMR spectra was recorded by adding HFIP in the solution of **HT3** in acetone-*d6*. We observed a downfield shift of two N–H peaks (Fig. 4c). This may be due to the possibility of several H-bonding modes between HFIP and **HT3**. In the same mixture, when nitrobenzene was added, it was noted that characteristic peaks shifted unequally in the downfield region. This is due to the possible interaction between –OH proton of HFIP with lone pair of oxygen in **HT3** that increase the N–H bond length and results in enhancement of H-bond donation of **HT3**. All these experiments suggest a plausible involvement of hydrogen bonding in this particular reaction. A case study was performed to compare the regioselectivities achieved in this H-bonding methodology and that achieved under our

https://doi.org/10.1038/s41467-024-51764-1

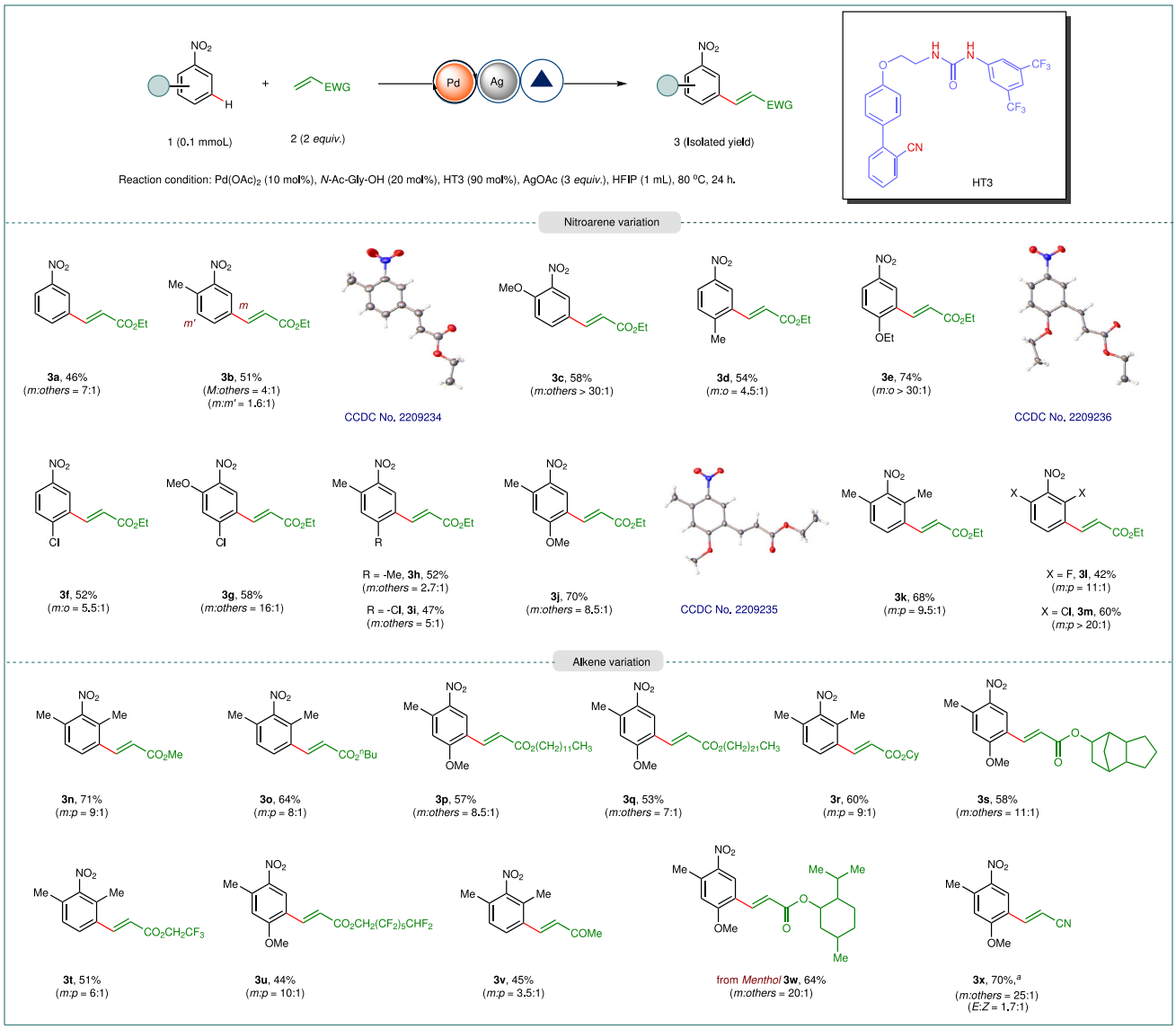

Fig. 3 | Substrate scope of nitroarenes and alkenes. [a]Yield and selectivity were determined from the ^{1}H NMR of the crude reaction mixture.

previously explored photo-redox condition (Fig. 4d)[27]. It was found that under photo condition, simple nitrobenzene gives better regioselectivity compared to the hydrogen bonding approach. However, we observed that the photoinduced alkenylation approach failed completely in case of the substituted nitrobenzenes. This shows the advantage of our H-bonding alkenylation protocol where several substituted nitroarenes can be functionalized at distal *meta*-position. In pursuit of a deeper understanding at the mechanistic level, our subsequent approach aimed to identify the pivotal phase that governs the pace of the nitroarene alkenylation reaction. For this purpose, we conducted simultaneous reactions utilizing both nitrobenzene and *d5*-nitrobenzene as substrates, adhering to established conditions (Fig. 4e). By assessing the initial rates and deducing the kinetic isotope effect (KIE) (k_H/k_D), a value of 1.2 was obtained. This observation strongly implies that the C−H activation step is improbable to serve as the rate-determining step in this reaction[28]. We have also attempted to find the reactivity of deuterated substrate in the absence of H-bonding template. It was noticed that deuterated nitrobenzene did not react up to two hours in the absence of template (Fig. 4f). As in the absence of template there is a significant difference in reactivity between nitrobenzene and *d5*-nitrobenzene, it clearly demonstrates that the C−H activation step is actually accelerated by the H-bonding template (Fig. 4f). In order to demonstrate the practicality of our protocol, we have scaled up this alkenylation reaction by taking 2,6-dimethyl nitrobenzene as a model substrate (Fig. 4g). The alkenylated product was formed with 54% yield without compromising the regioselectivity. The template (**HT3**) was also recovered from the reaction medium and recrystallized with 81% yield.

Computational studies

To obtain a detailed insight into the overall reaction mechanism, rate- and selectivity-determining steps, and the specific role of hydrogen bonding template (**HT**), we turned to density functional theory (DFT)-based calculations. The well-accepted density functional B3LYP (Becke's three-parameter exchange with Lee–Yang–Parr correlation) was employed for the DFT calculations for palladium-catalyzed reactions[29,30]. A detailed description of the computational methodology can be found in the Supplementary Information (page 46–57, Supplementary Information). We used the basic information on the catalytic cycle based on previous literature reports of palladium catalyzed distal C−H olefination[31], as a guide for our computational investigation. Specifically, the reaction involves five major steps:

https://doi.org/10.1038/s41467-024-51764-1

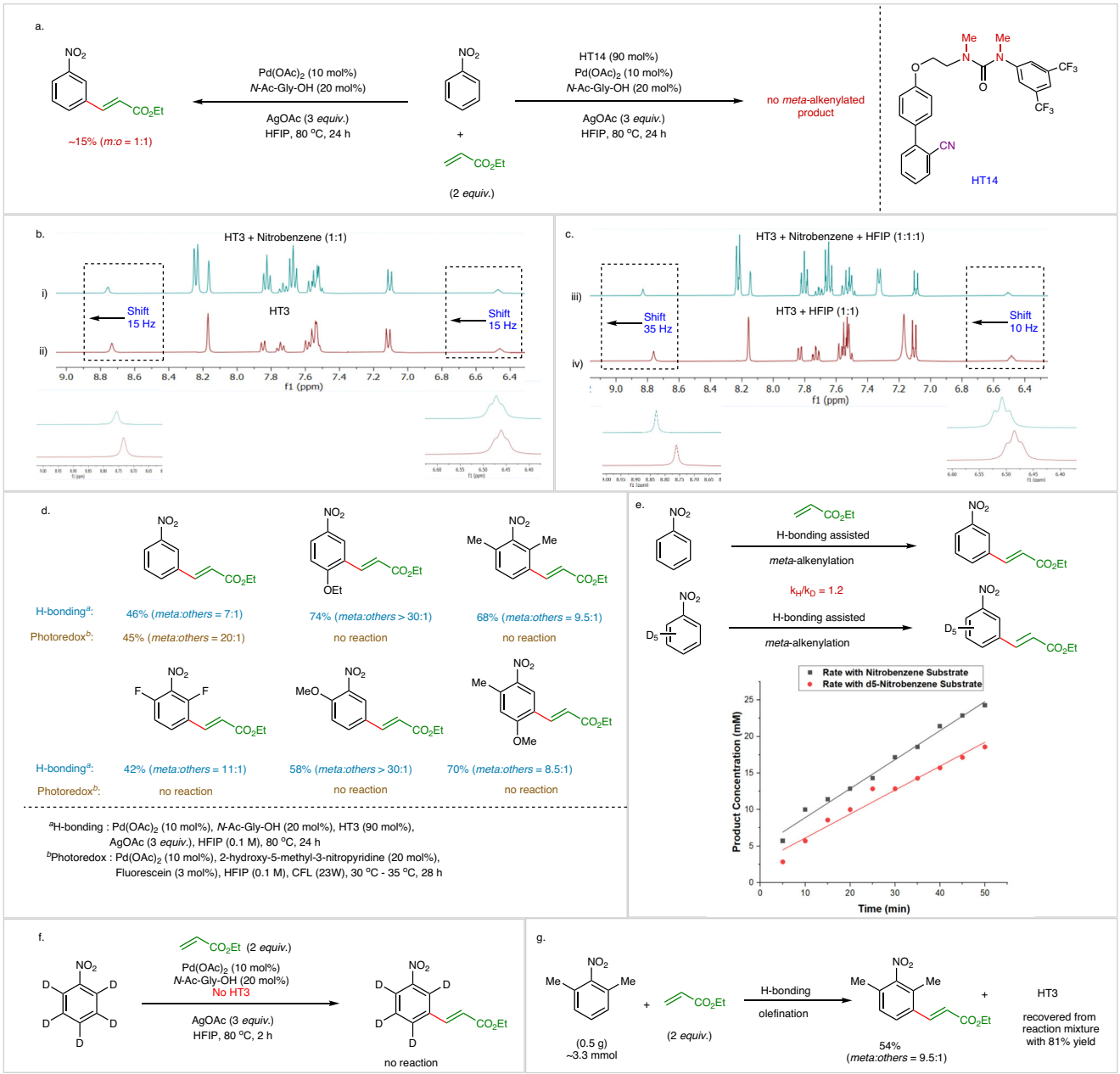

Fig. 4 | Mechanistic investigations for *meta*-C–H alkenylation of nitroarenes. **a** Control experiments. **b** (i) ^{1}H-NMR of the equimolar mixture of nitrobenzene and **HT3** in acetone-d_6. (ii) ^{1}H-NMR of **HT3**. **c** (iii) the mixture of HFIP, nitrobenzene and **HT3**. (iv) the mixture of HFIP and **HT3**. **d** Comparison of yield and regioselectivity between non-directed photo-redox reaction and hydrogen bonding approach. **e** Kinetic Isotope effect studies of Nitrobenzene. **f** Attempted alkenylation of deuterated nitrobenzene without template. **g** Up-scaled reaction and recovery of H-bonding template.

(i) activation of the N–H bond of *N*-acetyl glycine by acetate ligand of palladium acetate, (ii) activation of the *meta*-C–H bond of nitrobenzene by the *N*-acetyl glycine ligand of active catalyst, (iii) coordination and 1,2-migratory insertion of the alkene (iv) β-hydride elimination, and finally (v) reductive elimination followed by the product release. Figure 5 represents a stepwise reaction Gibbs free energy (ΔG) profile computed at the DFT-B3LYP level of theory. In the first step, the *N*-acetyl glycine coordinated Pd(II)-acetate complex (**RC**) undergoes N–H bond activation in the glycine unit by the acetate group through a facile barrier of 5.0 kcal/mol (**TS1**) that leads to the formation of **Int1**. In the subsequent step, the removal of AcOH followed by the co-ordination of substrate(nitrobenzene)-bound H-bonding template (**HT3**) generates **Int1'** in an endergonic binding process (ΔG = 10.4 kcal/mol). In **Int1'** the H-bonding template orients the *meta*-C–H bond of the nitrobenzene substrate close to the Pd-center, which triggers the C–H bond activation through a concerted metalation deprotonation (CMD)-type mechanism. The process leads to a palladacycle complex (**Int2**) that involves an overall free energy barrier of 17.4 kcal/mol with a six-membered transition state (**TS2**). To verify whether **TS2** is associated with the lowest energy C–H activation pathway, three different orientations of the substrate leading to three possible C–H activation pathways were investigated (Supplementary Fig. 14). Indeed, the pathway where the *N*-acetyl glycine ligand assists in activating the *meta*-C–H bond due to the coplanarity of the involved atoms was calculated to possess the lowest barrier. The other two pathways involve a much higher free energy barrier, 27.1, and 27.4 kcal/mol, respectively, and therefore, were discarded from our discussion (Supplementary Fig. 14). As the reaction moves past the C–H activation

https://doi.org/10.1038/s41467-024-51764-1

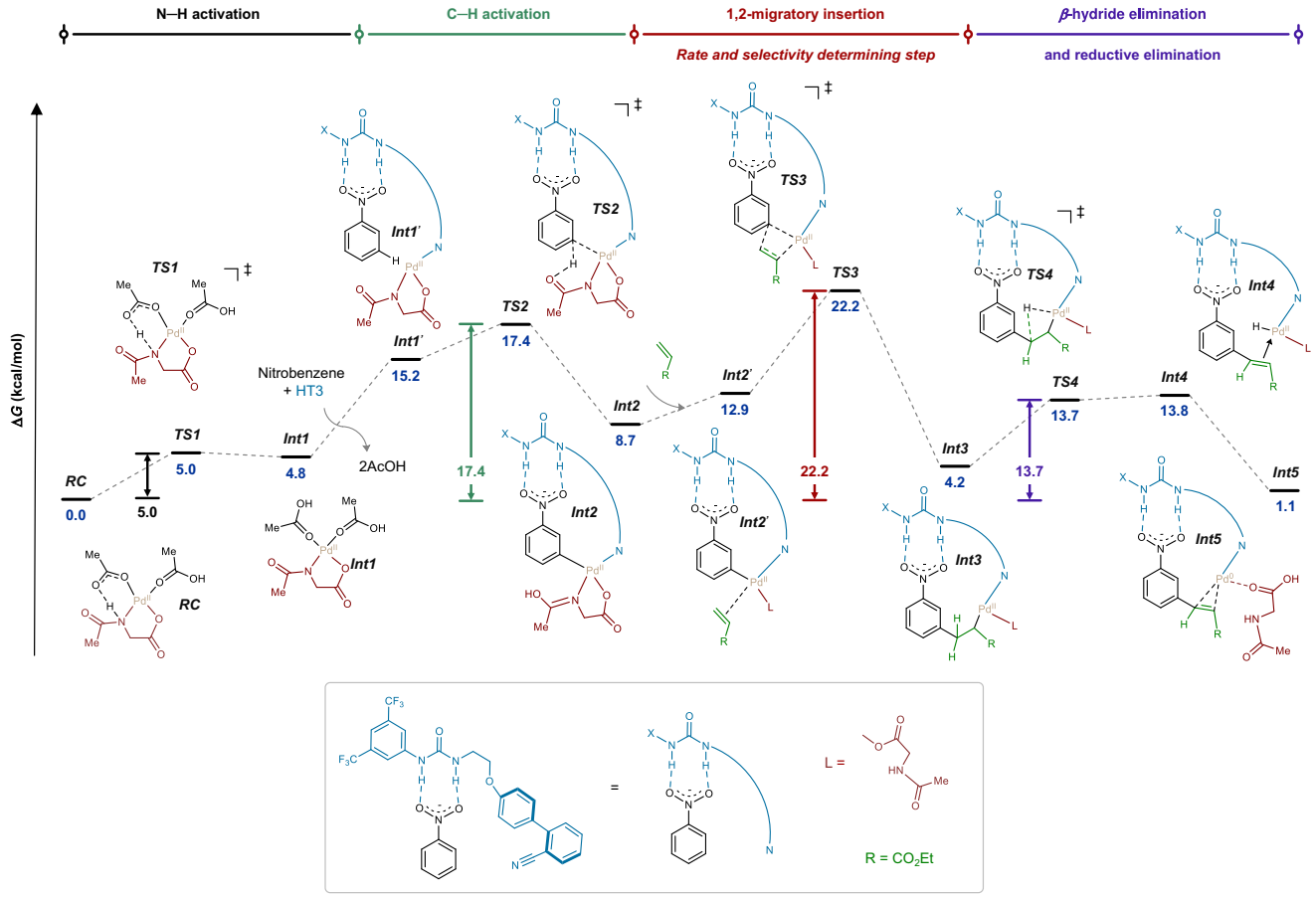

Fig. 5 | Gibbs free energy profile. Reaction Gibbs free energy profile for *meta*-C–H alkenylation of nitrobenzene evaluated at DFT-B3LYP-D3/Def2-QZVPP/SMD level of theory.

step, the alkene coordinates with the Pd(II)-center in **Int2**, and the resulting intermediate **Int2'** undergoes 1,2-migratory insertion of alkene to the Pd–C bond with an overall barrier of 22.2 kcal/mol through a highly strained four-membered transition state (**TS3**). We also considered the possibility of *N*-Ac-Gly-OH influencing or participating in the H-bonding strategy through the oxidative addition of alkene to Pd(II)-intermediate (**Int2**) resulting in a Pd(IV)-intermediate (Supplementary Fig. 15). However, the formation of a Pd(IV)-intermediate with an uncoordinated H-bonding template involves very high Gibbs free energy (ΔG = 26.3 kcal/mol), which lies even higher than the migratory insertion TS. Therefore, this possibility was discarded. In the subsequent step of the migratory insertion, an alkene-coordinated palladium(II)-hydride intermediate (**Int4**) is generated through the β-hydride elimination pathway, which involves a moderate free energy barrier of 13.7 kcal/mol (**TS4**). Finally, the palladium(II)-hydride intermediate undergoes reductive elimination at the Pd-center to form **Int5** featuring a Pd(0) center. The alkenylated product remains very weakly coordinated at the Pd(0) center in **Int5**, which gets released in the subsequent step. The silver acetate present in the reaction re-oxidizes the Pd(0) metal center to Pd(II), thereby, regenerating the Pd(II)-based active catalyst. As per the stepwise reaction energetics presented above, the 1,2- migratory insertion step possessing the highest overall free energy barrier ($\Delta G^{\ddagger}$ = 22.2 kcal/mol) among the four key reaction steps appeared to be the rate-determining step (RDS) of the overall reaction. Thus, the C–H activation step with an appreciably lower barrier ($\Delta G^{\ddagger}$ = 17.4 kcal/mol) is not involved in the RDS. This computational finding appears consistent with the experimental observation of a KIE value of 1.2 obtained through the parallel reaction method. To justify the role of the H-bonding template, the entire reaction energetics involving four key reaction steps was computed without the template (Supplementary Fig. 16). In this case, the C–H activation step was calculated to involve the highest free energy barrier with a very high value of 32.1 kcal/mol. Moreover, the 1,2-migratory insertion step also involves a very high barrier of 27.4 kcal/mol. Therefore, the highest barrier, which is ~10 kcal/mol higher as compared to the reaction pathway assisted by the H-bonding template, clearly showcases the significant accelerating effect on the alkenylation reaction. To answer the question of why **HT3** turned out to be the optimal one among the three reactive templates (**HT1**, **HT2**, and **HT3**), as observed during the experimental reaction optimization process, we performed a side-by-side analysis of the free energy barrier and electronic effects of the critical C–H activation step participated by **HT1**, **HT2**, and **HT3** (Supplementary Fig. 17). As borne out from our calculations, **HT3** due to its structural flexibility could align both the –NH donors toward the acceptor $-NO_2$ group of the substrate, and thereby, form two H-bonds. On the other hand, **HT1** and **HT2** could only manage one H-bond due to the structural reservation. The H-bonds were clearly visible through the NCI analysis presented in Supplementary Fig. 17b. Consequently, **HT3** undergoes the C–H activation step with a much lower barrier of 17.4 kcal/mol as compared to **HT1** and **HT2** both showing a barrier of 23.2 and 21.9 kcal/mol respectively. A similar effect was observed for the rate-determining 1,2-migratory insertion step involving **TS3** (Supplementary Fig. 18). To shed light on the regioselectivity enforced by **HT3**, geometric and electronic analysis of the transition state that is involved in the RDS step (**TS3**) was performed. Three different transition states leading to *meta* (*m*-**TS3**), *para* (*p*-**TS3**), and *ortho* (*o*-**TS3**) C–H alkenylation selectivity of the nitrobenzene substrate were computed (Fig. 6). It is apparent that the hydrogen-bonding interactions

https://doi.org/10.1038/s41467-024-51764-1

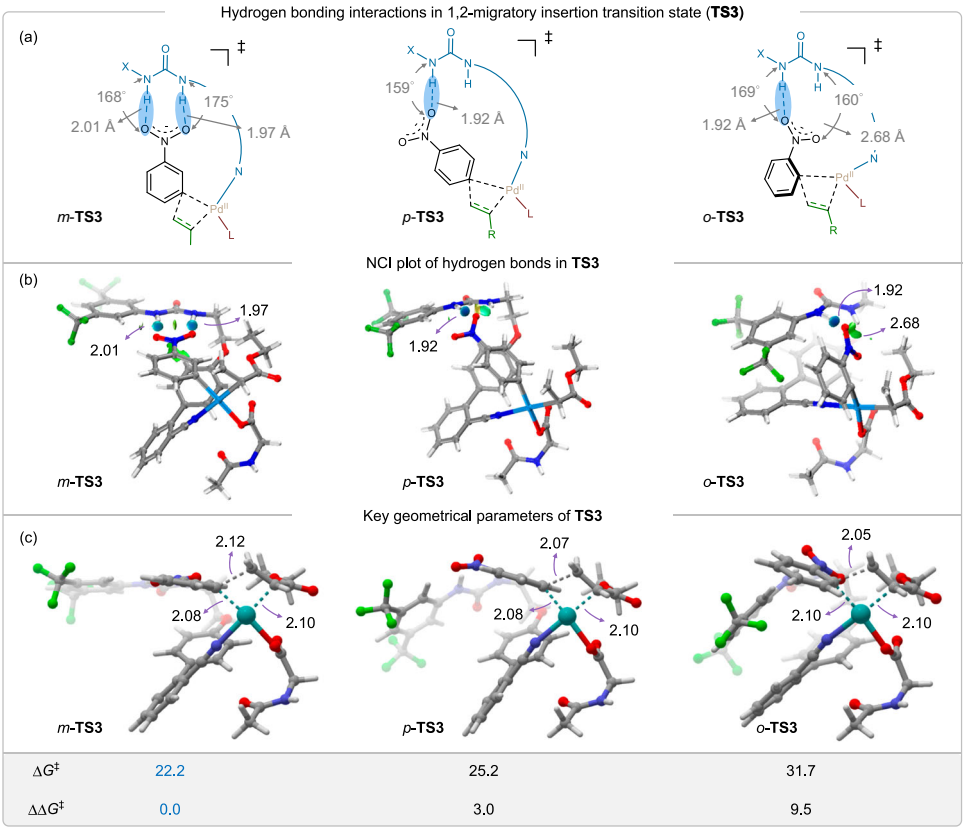

Fig. 6 | Origin of regioselectivity through hydrogen bonding interactions in RDS. a Key geometrical parameters of hydrogen-bonding interactions in 1,2-migratory insertion TS (**TS3**), **b** NCI plots indicating hydrogen bonds (the disks in the NCI plot denotes H-bonds), and **c** key geometrical parameters of the *meta*-, *para*-, and *ortho*- selective **TS3**.

between the nitro group of the substrate and the –NH group of the template exert a stabilization effect that lowers the energy of the TSs as well as the intermediates. A careful inspection of the *meta*-selective transition state (*m*-**TS3**) geometry unravels that there is a formation of two hydrogen bonds between two optimally aligned donors –NH groups of **HT3** and two acceptor O-atoms of the nitrobenzene substrate with hydrogen-bonding distances of 2.01 Å and 1.97 Å in an almost linear fashion (∠NHO = 168°) (Fig. 6a). On the contrary, the *para*- and *ortho*-selective transition state (*p*-**TS3** and *o*-**TS3**) feature only one H-bond (1.92 Å) between the –NH group of **HT3** and the O-atom of the nitro group. Consequently, the Gibbs free energy barriers for the later cases of *p*-**TS3** ($\Delta G^{\ddagger}$ = 25.2 kcal/mol) and *o*-**TS3** ($\Delta G^{\ddagger}$ = 31.7 kcal/mol) were calculated to be appreciably higher as compared to the *m*-**TS3** ($\Delta G^{\ddagger}$ = 22.2 kcal/mol). The H-bonding interactions were also clearly evidenced through the non-covalent interaction (NCI) plots (Fig. 6b). Therefore, the relative Gibbs free energy of the other transition states, *p*-**TS3** ($\Delta\Delta G^{\ddagger}$ = 3.0 kcal/mol) and *o*-**TS3** ($\Delta\Delta G^{\ddagger}$ = 9.5 kcal/mol), with respect to *m*-**TS3** nicely demonstrates the prevailing *meta*-selectivity effect (*m*:*others* = 7:1, Fig. 3) of the H-bonding template. In line with this selectivity rationalization, we further analyzed the impact of aromatic-ring substituent on the selectivity. For this purpose, substrate **3e**, containing *para*-OEt substitution and **3 h** with 2,4-dimethyl substitution were selected. The highest selectivity observed for **3e** (*m*:*others* > 30:1, Fig. 3) can be attributed to the formation of a much stronger hydrogen bond in *meta*-**TS3** due to the enhancement of the electron density on the $-NO_2$ group of nitrobenzene by electron-donating –OEt group. This stabilizes the rate-determining TS ($\Delta G^{\ddagger}$ = 19.4 kcal/mol, Supplementary Fig. 19) by ~3.0 kcal/mol relative to the unsubstituted nitrobenzene containing *m*-**TS3** ($\Delta G^{\ddagger}$ = 22.2 kcal/mol, Fig. 6). On the other hand, the transition state of the only other isomer i.e., *ortho*-**TS3** is destabilized due to the involvement of only one O-atom of the nitro group towards hydrogen bonding (Supplementary Fig. 19). This leaves a large barrier difference between *meta*-**TS3** and *ortho*-**TS3** with $\Delta\Delta G^{\ddagger}$ of 10.9 kcal/mol and highly favoring the formation of the *meta*-alkenylated product over the *ortho*-alkenylated product. For the same reason, the lowest selectivity was observed for 2,4-dimethyl substituted nitrobenzene (**3h**), which is reflected through a small difference between the activation barrier of rate-determining *meta*- and *ortho*-**TS3** ($\Delta\Delta G^{\ddagger}$ = 3.9 kcal/mol, Supplementary Fig 20). We further investigated the accelerating effect of the H-bonding template in the C–H activation (**TS2**) and β-hydride elimination (**TS4**) steps. As shown in Supplementary Fig. 21 of the Supplementary Information, both the H-bonds between the –NH donors and $-NO_2$ acceptor remain intact throughout the reaction course, as consistently observed in **TS2**, **TS3**, and **TS4** (Supplementary Fig 21)[32]. This observation further strengthens the critical role of the H-bonding template in the *meta*-selective C–H alkenylation reaction. Finally, to evaluate the role of the mono-protected amino acid (MPAA) ligand in the overall reaction, the Gibbs free energy barrier of the crucial C–H activation and 1,2-migratory insertion steps were calculated with four different types of ligands **L1**-**L4** (Supplementary Figs. 22 and 23). It was anticipated that bulkier ligands would exert a steric effect around the Pd-center and destabilize the corresponding transition state. This was, indeed, observed in both the cases of **TS2** (Supplementary Fig. 22) and **TS3** (Supplementary Fig. 23). In the first case, i.e., for the C–H activation step (**TS2**), relatively bulkier ligands (**L2**-**L4**) introduce non-planarity in the six-membered transition state, and thereby, enhance the reaction barrier by 2.1, 6.9, and 6.7 kcal/mol for **L2**, **L3**, and **L4**, respectively as compared to the optimal ligand **L1** (Supplementary Fig. 22)[33]. A similar,

but less pronounced effect was observed in the case of **TS3**, where the bulkier ligands **L2**-**L4** involve a larger barrier ranging ~0.5–3.5 kcal/mol relative to **L1** (Supplementary Fig. 23).

In summary, palladium-catalyzed distal *meta*-alkenylation of nitroarenes through the incorporation of urea-based hydrogen bonding has been accomplished. Notably, a diverse range of nitrobenzenes has demonstrated remarkable suitability within this framework. Our findings are supported by an array of control experiments, NMR analysis, and meticulous DFT-based mechanistic studies which affirm the existence of hydrogen bonding interactions between the substrate and the template. The experimentally observed selectivity could be nicely rationalized through the relative Gibbs free energy barriers of different transition states involved. In our pursuit of unraveling the reaction's complexities, we undertook kinetic investigations and conducted an in-depth computational mechanistic analysis. As a result, we identified the 1,2-migratory insertion as the rate-determining step, intricately by the participation of the hydrogen-bonding template. The pivotal role played by the extended biphenyl spacer-based hydrogen bond donor template, combined with the employed ligand, holds substantial promise for a broader spectrum of synthetic applications.

Methods

General procedure for the synthesis of alkenylated nitroarenes

A clean, oven-dried screw cap reaction tube with previously placed magnetic stir–bar was charged with Nitroarene (0.1 mmol, 1 *equiv.*), alkene partner (0.2 mmol, 2 *equiv.*), $Pd(OAc)_2$ (0.01 mmol, 10 mol%), *N*-Ac-Gly-OH (0.02 mmol, 20 mol%), H-bonding template (**HT3**) (0.09 mmol, 90 mol%) and AgOAc (0.3 mmol, 3 *equiv.*) followed by addition of HFIP (1 mL). The reaction mixture was vigorously stirred for 24 hours in a preheated oil bath at 80 °C. After stipulated time, the reaction mixture was cooled to room temperature and filtered through a celite bed. The crude reaction mixture was purified by column chromatography using silica gel and petroleum-ether/ethyl acetate as the eluent to give the desired alkenylated-nitroarene as the product.

Data availability

Details about materials and methods, experimental procedures, mechanistic studies, characterization data, and NMR spectra are available in the Supplementary Information. Additional data are available from the corresponding author upon request. Crystallographic data are available from the Cambridge Crystallographic Data Centre of the following compounds: 3b (CCDC 2209234), 3e (CCDC 2209236), 3j (CCDC 2209235) and HT3 (CCDC 2209378). These data can be obtained free of charge from https://www.ccdc.cam.ac.uk/data_request/cif. Source data are provided with this paper.

References

1. Tang, R., Li, G. & Yu, J.-Q. Conformation-induced remote *meta*-C–H activation of amines. *Nature* **507**, 215–220 (2014).
2. Bera, M., Modak, A., Patra, T., Maji, A. & Maiti, D. *Meta*-Selective Arene C–H Bond Olefination of Arylacetic Acid Using a Nitrile-Based Directing Group. *Org. Lett.* **16**, 5760–5763 (2014).
3. Bag, S. et al. Remote *para*-C–H Functionalization of Arenes by a D-Shaped Biphenyl Template-Based Assembly. *J. Am. Chem. Soc.* **137**, 11888–11891 (2015).
4. Leow, D., Li, G., Mei, T.-S. & Yu, J.-Q. Activation of remote *meta*-C–H bonds assisted by an end-on template. *Nature* **486**, 518–522 (2012).
5. Yang, G. et al. Pd(II)-Catalyzed *meta*-C–H Olefination, Arylation, and Acetoxylation of Indolines Using a U-Shaped Template. *J. Am. Chem. Soc.* **136**, 10807–10813 (2014).
6. Bag, S. et al. Imine as a linchpin approach for *meta*-C–H functionalization. *Nat. Comm.* **12**, 1393 (2021).
7. Goswami, N., Bhattacharya, T. & Maiti, D. Transient directing ligands for selective metal-catalysed C–H activation. *Nat. Rev. Chem.* **5**, 646–659 (2021).
8. Liu, X.-H. et al. Diverse *ortho*-C(sp2)–H Functionalization of Benzaldehydes Using Transient Directing Groups. *J. Am. Chem. Soc.* **139**, 888–896 (2017).
9. Das, S., Incarvito, C. D., Crabtree, R. H. & Brudvig, G. W. Molecular recognition in the selective oxygenation of saturated C–H bonds by a dimanganese catalyst. *Science* **312**, 1941–1943 (2006).
10. Davis, H. J. & Phipps, R. J. Harnessing non-covalent interactions to exert control over regioselectivity and site-selectivity in catalytic reactions. *Chem. Sci.* **8**, 864–877 (2017).
11. Kuninobu, Y., Ida, H., Nishi, M. & Kanai, M. A *meta*-selective C–H borylation directed by a secondary interaction between ligand and substrate. *Nat. Chem.* **7**, 712–717 (2015).
12. Davies, H. J., Mihai, M. T. & Phipps, R. J. Ion pair-directed regiocontrol in transition-metal catalysis: a *meta*-selective C–H borylation of aromatic quaternary ammonium salts. *J. Am. Chem. Soc.* **138**, 12759–12762 (2016).
13. Yang, L., Uemura, N. & Nakao, Y. *M*eta-selective C–H borylation of benzamides and pyridines by an iridium–Lewis acid bifunctional catalyst. *J. Am. Chem. Soc.* **141**, 7972–7979 (2019).
14. Hoque, E., Bisht, R., Haldar, C. & Chattopadhyay, B. Noncovalent interactions in Ir-catalyzed C–H activation: L-shaped ligand for *para*-selective borylation of aromatic esters. *J. Am. Chem. Soc.* **139**, 7745–7748 (2017).
15. Lu, S. et al. *para*-Selective C–H Borylation of Aromatic Quaternary Ammonium and Phosphonium Salts. *Angew. Chem. Int. Ed.* **61**, 1–5 (2022).
16. Cheng, W. et al. Computationally designed ligands enable tunable borylation of remote C–H bonds in arenes. *Chem* **8**, 1775–1788 (2022).
17. Li, G., Yan, Y., Zhang, P., Xu, X. & Jin, Z. Palladium-Catalyzed *meta*-Selective C–H Functionalization by Noncovalent H-Bonding Interaction. *ACS Catal.* **11**, 10460–10466 (2021).
18. Goswami, N. et al. Non-Covalent Interaction within Catalytic Anionic Donor and Neutral Acceptor to Promote Pd-Catalyzed Distal Site-Selective Functionalization of Amines. *Chem* **9**, 1–15 (2023).
19. Mondal, A., Diaz-Riaz, M., Deufel, F., Maseras, F. & van Gemmeren, M. Charge-controlled Pd catalysis enables the *meta*-C–H activation and olefination of arenes. *Chem* **9**, 1–13 (2023).
20. Zheng, Y.-H., Shi, B.-F. & Yu, J.-Q. Pd(II)-catalyzed olefination of electron-deficient arenes using 2, 6-dialkylpyridine ligands. *J. Am. Chem. Soc.* **131**, 5072–5074 (2009).
21. Mąkosza, M. & Wojciechowski, K. Nucleophilic substitution of hydrogen in heterocyclic chemistry. *Chem. Rev.* **104**, 2631–2666 (2004).
22. Bartoli, G., Dalpozzo, R. & Nardi, M. Applications of Bartoli indole synthesis. *Chem. Soc. Rev.* **43**, 4728–4750 (2014).
23. Tan, E., Montesinos-Magraner, M., Garc´ıa-Morales, C., Mayans, J. G. & Echavarren, A. M. Rhodium-catalysed *ortho*-alkynylation of nitroarenes. *Chem. Sci.* **12**, 1473–14731 (2021).
24. Peng, M. et al. Bond Activation, Alkyne Insertion, and Rearrangements by Rh(III)-Catalysis: Oxindole Synthesis from Nitroarenes and Alkynes. *J. Am. Chem. Soc.* **145**, 4508–4516 (2023).
25. Luo, T., Vohs, J. M. & Gorte, R. J. An Examination of Sulfur Poison-ing on Pd/Ceria Catalysts. *J. Cat.* **210**, 397–404 (2002).
26. Bhattacharya, T., Ghosh, A. & Maiti, D. Hexafluoroisopropanol: The magical solvent for Pd-catalyzed C–H activation. *Chem. Sci.* **12**, 3857–3870 (2021).
27. Saha, A. et al. Photoinduced regioselective olefination of arenes at proximal and distal sites. *J. Am. Chem. Soc.* **144**, 1929–1940 (2022).
28. Simmons, E. M. & Hartwig, J. F. On the Interpretation of Deuteri-um Kinetic Isotope Effects in C–H Bond Functionalizations by Transition-Metal Complexes. *Angew. Chem. Int. Ed.* **51**, 3066–3072 (2012).

29. Fan, Z. et al. Rational development of remote C–H functionalization of biphenyl: Experimental and computational studies. *Angew. Chem. Int. Ed.* **59**, 4770–4777 (2020).
30. Bag, S. et al. Palladium-Catalyzed *meta*-C–H Allylation of Arenes: A Unique Combination of a Pyrimidine-Based Tem-plate and Hexafluoroisopropanol. *J. Am. Chem. Soc.* **142**, 12453–12466 (2020).
31. Ali, W., Prakash, G. & Maiti, D. Recent development in transition metal-catalysed C–H olefination. *Chem. Sci.* **12**, 2735–2759 (2021).
32. Reek, J. N. H. et al. Transition metal catalysis controlled by hydrogen bonding in the second coordination sphere. *Chem. Rev.* **122**, 12308–12369 (2022).
33. Cheng, G.-J. et al. Role of *N*-Acyl Amino Acid Ligands in Pd(II)-Catalyzed Remote C–H Activation of Tethered Arenes. *J. Am. Chem. Soc.* **136**, 894–897 (2014).

Acknowledgements

Financial support received from SERB-CRG, India is gratefully acknowledged (CRG/2022/004197). We acknowledge the financial support from the SERB Start-up Research Grant (SRG/2020/000691) and from IIT Mandi Seed Grant (IITM/SG/ABP/76). Financial support received from PMRF-MHRD (fellowship to B.D.), CSIR-India (fellowship to A.G.), IIT Bombay is gratefully acknowledged. M.M. is thankful to the Ministry of Education (MoE) for the research fellowship. High-Performance Computing (HPC) facility at IIT Mandi and National Supercomputing Mission (NSM) for providing computing resources of 'PARAM Himalaya' at IIT Mandi, which is implemented by C-DAC and supported by the Ministry of Electronics and Information Technology (MeitY) and Department of Science and Technology (DST), Government of India are gratefully acknowledged. National Science Center, Poland is acknowledged for financial support (Grant No. 2016/22/E/ST5/00046) for R.K. and M.D. H.G. acknowledges NSF (CHE-2029932), the Robert A. Welch Foundation (D-2034-20230405), and Texas Tech University for financial support. We thank Mr. Sukumar Pradhan for his generous help.

Author contributions

B.D., A.G., R.K. and D.M. conceived the concept. M.D. synthesized all the squaramide-based hydrogen bonding templates. B.D. and A.G. synthesized all the urea and thiourea-based hydrogen bonding templates. B.D. performed the final reactions and analyzed the products. M.M. and B.M. designed and performed all the computational studies and analyzed the results. A.G. performed X-ray diffraction analysis and analyzed the structure. B.D., M.M., B.M., R.K., H.G. and D.M. wrote the manuscript.

Competing interests

The authors declare a competing financial interest. D.M., B.D. and A.G. are named as inventors on a patent application filed by the Indian Institute of Technology Bombay based on the work described in this manuscript; application number 202321079920. The authors declare no other financial or non-financial competing interests.

Additional information

Supplementary information The online version contains supplementary material available at https://doi.org/10.1038/s41467-024-51764-1.

Correspondence and requests for materials should be addressed to Rafal Kowalczyk, Bhaskar Mondal, Haibo Ge or Debabrata Maiti.

Peer review information *Nature Communications* thanks Yu-Peng He and the other anonymous reviewer(s) for their contribution to the peer review of this work. A peer review file is available.